A Novel Ultra-Broadband DC-36-to-66-GHz Hybrid Diplexer Using Waveguide and SSL Technology

Irfan Ashiq, Amarpal Khanna
Microwave Components
National Instruments Santa Clara, CA USA
iashiq@ni.com, pkhanna@ni.com

***Abstract*—This paper describes a novel wideband low-loss contiguous diplexer with steep band selectivity achieved by combining a planar suspended stripline (SSL) and waveguide filter. The diplexer is comprised of an input circuit configured to receive a broadband signal, a low-pass filter (LPF), and a high-pass filter (HPF) and covers DC 36 to 66 GHz. The LPF is implemented using a planar transmission line. The HPF is implemented using a waveguide and is connected to the LPF using a SSL-to-waveguide transition.**

Keywords—hybrid diplexer, suspended stripline, contiguous diplexer, soft-board, recessed cavity, lowpass filter, highpass filter, millimeter wave diplexer, SSL to waveguide transition.

I. INTRODUCTION

Diplexers using either planar (i.e., microstrip or SSL) or non-planar (i.e., waveguide) transmission lines have been presented before [1], [2]. The wideband diplexer presented in this paper introduces a new concept of combining planar and non-planar filters for the first time in a configuration we call "Hybrid diplexer." The design lends itself well to broadband systems working in the millimeter-wave frequency range and higher where filter loss and etching tolerances associated with planar designs can become impractical. Combining planar and waveguide filters enables diplexer design to be easily implemented in E band and W band [2].

This wideband contiguous hybrid diplexer includes a planar LPF that connects to the high-pass-waveguide filter through a transition probe at the input common junction. The combination of waveguide and SSL also has ~~some~~ additional attractive features compared to conventional microstrip and stripline filters. These features include better temperature stability, less dispersion, flatter group delay, and lower loss over a wider frequency bandwidth. The planar substrate material used is RO5880 has a dielectric constant of 2.1 and an effective dielectric constant of 1.1 as a result of the SSL structure.

One applications for such a wideband diplexer is the RF front-end of high-frequency real-time oscilloscopes. The diplexer in fig. 1 separates the incoming signal into two frequency bands (DC to 36 GHz and 36 GHz to 65 GHz.) The higher frequency band is block down-converted to a frequency range suitable for acquisition by digitizing channels [4]. In digital bandwidth interleaving (DBI) systems, the digitized bands (higher and lower) are then stitched back to re-create the time domain signal.

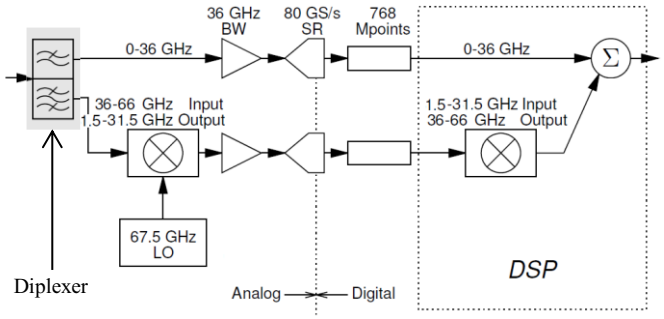

Fig. 1 Digital bandwidth interleaving (DBI) system block diagram [4]

II. DIPLEXER DESIGN

A. SSL design and higher order modes

Figure 2 shows a SSL cross-sectional view of a 0.005-inch dielectric substrate housed in a proportional, recessed air cavity enclosed in a shielded rectangular waveguide.

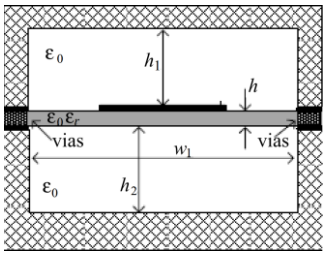

Fig. 2. 2D model of the lowpass section of the diplexer

The input and LPFs are implemented on a SSL. The height ($=h_1+h_2+h$) and width (w_1) of the SSL cavity are optimized such that the higher order TE and TM hybrid modes are suppressed below intended frequencies of operation [3]. For the dominate mode to be quasi TEM in the SSL structure, the cut-off frequency of the loaded SSL is set to be above 66 GHz and can be computed with equation below:

$$f_c = \frac{c}{2w_1}\sqrt{1-\frac{h}{b}\left(\frac{\epsilon_r-1}{\epsilon_r}\right)} \qquad (1)$$

Where w_1 is the channel width, b is the channel height ($=h_1+h_2+h$), c is the speed of light, and h is the substrate height.

B. Diplexer model and synthesis

The design of the diplexer is split into two parts—LPFs and HPFs. The LPF of the diplexer is based on a conventional LC, 13 section Tchebyshev design implemented in the SSL. The highpass section of the diplexer is comprised of two sections, the SSL-to-waveguide transition and waveguide-to-SSL and coaxial transition. The entire design and optimization of the highpass-waveguide-filter design is conducted in a 3D EM simulator.

C. LPF

The Tchebyschev lowpass section of the diplexer is synthesized using the iFilter feature in AWR's Microwave Office. The cutoff frequency (f_0) of the filter is set to 36 GHz with a pass-band ripple of 0.1 dB. The 13th order stepped impedance lowpass design is synthesized by implementing series λ/8 high impedance (120 ohms) and shunt λ/2 low impedance (70 ohm) resonators. Figure 3 and 4 shows the E-M optimized LPF section and its response.

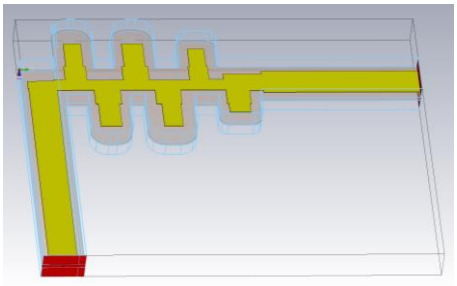

Fig. 3. 3D model of the lowpass section of the diplexer

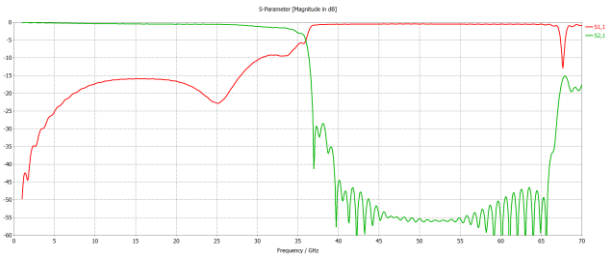

Fig. 4. Response of the highpass section of the diplexer

Some of the key dimensions of the LPF on the SSL include series inductive widths of 0.017 inches and shunt capacitive resonator widths of 0.02 inches. The 50-ohm tranmission line is optimized for a width of 0.035 inches.

D. HPF

The HPF is a true waveguide structure. The common input junction of the diplexer is connected to a resonator stub or a probe via a single capacitive broadside-coupled section implemented on a 0.005 inch dielectric substrate. This probe also acts as a transition from the SSL to rectangular waveguide. The input broadband signal is propagated in TEM mode in the SSL structure, which then converts to the dominant TE_{10} when launched through a probe into the waveguide as shown in fig. 5.

To ensure maximum energy transfer to the TE_{10} mode, the suspended probe was positioned in the middle of the waveguide with one end of the guide shorted. The distance of the probe to the back short is optimized. The electrical distance between the probe and the short needs to be one quarter of guide wavelength (at center of highpass frequency range) in order to maximize RF energy in the z+ direction. The depth of the probe also plays a critical role to ensure max energy is transitioned from the probe into waveguide the probe. For this design, the probe depth is chosen to be 0.6 times the waveguide height [2].

The a and b dimensions of the waveguide are chosen such that TE_{10} cutoff frequency of the guide is 36 GHz, calculated from equation (2) and the wave impedance computed from equation (3) [3].

$$f_{cTE10} = c/2a \tag{2}$$

$$Z_{TE10} = \frac{\sqrt{\frac{\mu}{\epsilon}}}{\sqrt{1-f_c^2/f^2}} > \sqrt{\frac{\mu}{\epsilon}} \tag{3}$$

The dimensions for the waveguide were chosen to be 0.082 x 0.164 inches. Since the dimensions are non-standard, a transition from a non-standard waveguide to the SSL and finally to a coaxial connector was designed to enable a complete broadband response from DC to 66 GHz [2]. Figures 5 and 6 show the model and the response of the HPF. Fig. 5 displays E-field energy flowing from the input to the waveguide of the HPF.

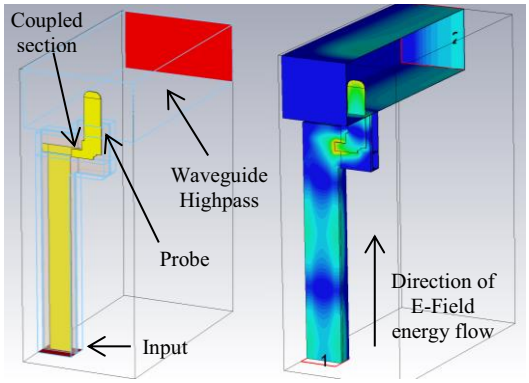

Fig. 5. 3D model of the highpass section of the diplexer on the left and cross-sectional view of excited TEM mode on the right

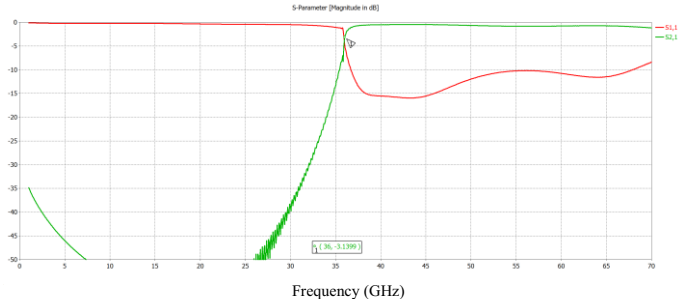

Fig. 6. Response of the highpass section of the diplexer

E. Simulation

The diplexer had design specifications that are shown in table 1.

Parameter	*Attenuation (dB)*	*Frequency range (GHz)*
$\|S_{11}\|$	≤ -10	DC-66 GHz
$\|S_{22}\|$	≤ -12	DC-36GHz
$\|S_{33}\|$	≥ -10	36-66 GHz
$\|S_{21}\|$	≤ -1	DC-36 GHz
$\|S_{31}\|$	≤ -2	36-66 GHz
$\|S_{21}\|$	≤ -6	At cross-over

TABLE I. DIPLEXER SPECIFICATIONS

The initial design step is to simulate a 13th order lumped-circuit-based model for the entire diplexer. Following the closed form circuit simulation, the lumped equivalent elements, were converted to transmission lines using a synthesis tool. For the hybrid diplexer design, the highpass-circuit-based model was replaced by a non-standard waveguide having a cutoff at the cross-over frequency. The final E-M optimized diplexer model was split into the following three sections: planar LPF, waveguide HPF, and waveguide-to-SSL transition.

The highpass section required a non-standard waveguide between WR-19 and WR-15 in order to cover the 36 GHz to 65 GHz frequency band. The waveguide-to-SSL transition is designed at the output of the waveguide highpass to meet design requirements of the DBI front-end.

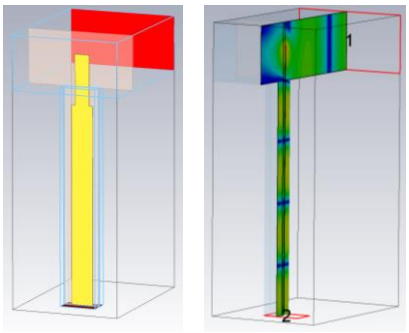

Fig. 7. Waveguide-to-SSL transition: TE to TEM mode propagation (left) and model (right)

The E-M optimized transition from the waveguide-to-SSL needed to be matched to achieve low loss and flatter response across the band. Figures 7 and 8 show the model and response of the hybrid diplexer's output transition. The complete model of the hybrid diplexer is shown in fig. 9. The comparison of the closed-form-circuit-based model versus the optimized E-M-based-model is shown in figure 10.

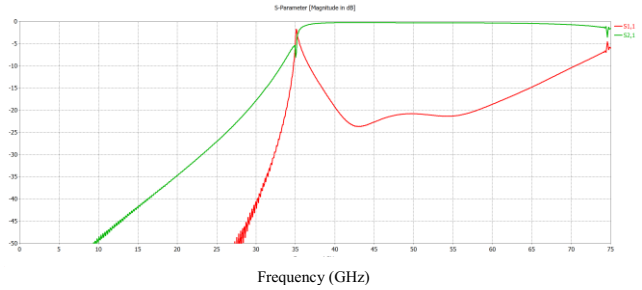

Fig.8. Response of the waveguide to SSL transition

Note that in fig. 10, the plot of the closed form diplexer simulation exhibits reduced band selectivity in comparison to the E-M based model.

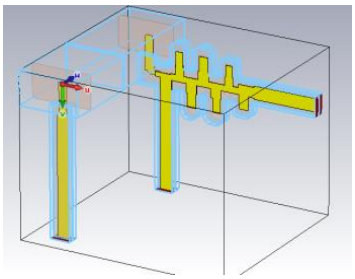

Fig. 9. 3D model of the hybrid diplexer with WG-to-SSL transition

The steep roll-off (S21 and S31) in the crossover region in the E-M model is due to the high quality factor of the SSL and the highpass waveguide.

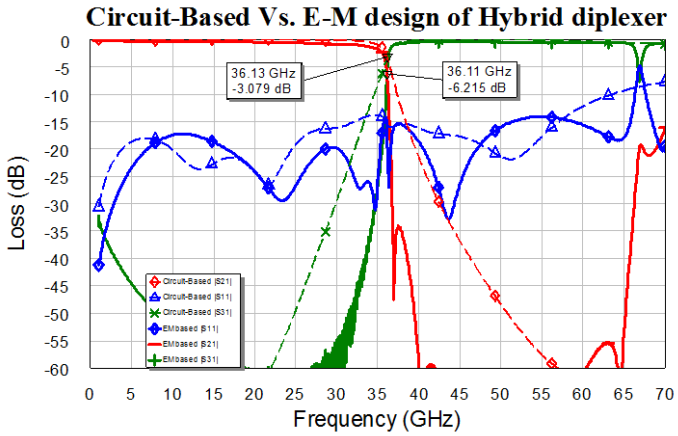

Fig. 10. Diplexer simulated response from DC to 70 GHz

F. Fabrication and machining

Gold-plated brass was used for the mechanical housing and recessed cavities. High-frequency microcircuits requires high-accuracy machining of the mechanical cavities and tight-tolerance etching of the PCB. Mechanical machining accuracies better than 0.0005 inches and PCB etch tolerances of better than 0.00075 inches were held in order to achieve a good correlation between simulated and the measured results. Figure 11 shows a completely assembled hybrid diplexer with

1.85 mm connectors mounted with four-hole flanges on all three ports. The overall size of the hybrid diplexer excluding the flange connectors is 0.8 x 0.5 x 0.7 inches.

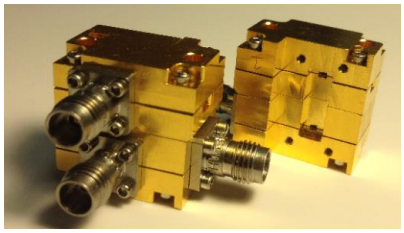

Fig.11. Assembled wideband DC-36-to-65-GHz hybrid diplexer

III. Measured Results

The measured result shown in fig. 12 displays excellent agreement between simulation and measured data. The passband ripple is less than 0.5 dB with 1.5 dB loss at 66 GHz. Crossover was at 36.75 GHz with an insertion loss of 6.5 dB. Both the LPF and HPF show very high rejection in the reject band. The measured response in fig. 12 is shown with final post tuning.

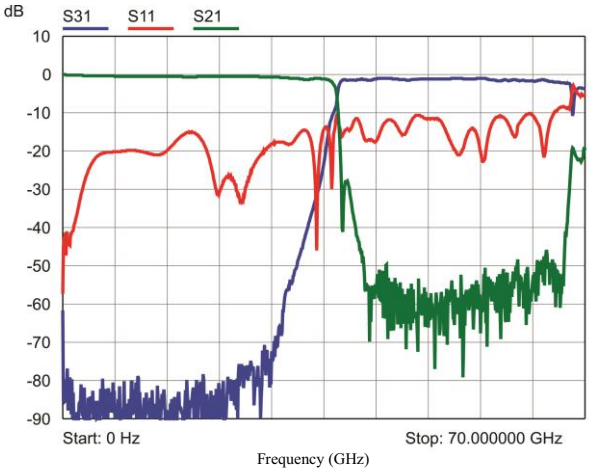

Fig. 12. Diplexer measured response from 10 MHz to 70 GHz

The diplexer exhibits a flatter group delay across the band as shown in figure 13 and 14. Figure 13 shows the measured group delay of the LPF section measured between lowpass and common port and is reported to be better than 100 picoseconds. One the other hand, figure 14 shows the measured group delay of the HPF section measured between highpass and common port to be better than 200 picoseconds between 40 GHz and 66 GHz. The peaking in group delay around the crossover region from 35 GHz to 38 GHz is due to the abrupt phase variation when transitioning from lowpass to highpass.

IV. Conclusion

A novel high-performance hybrid contiguous diplexer (covering DC to 36 to 66 GHz) by combining waveguide and SSL transmission lines is presented.

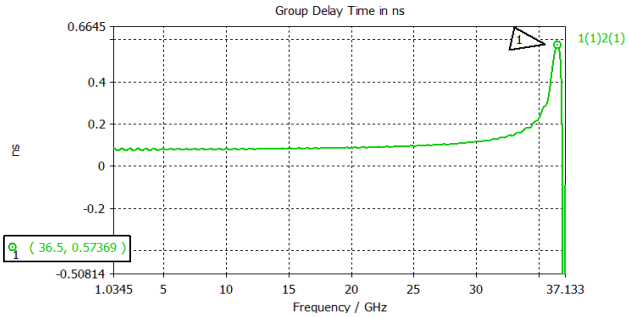

Fig. 13. Measured group delay from port 2 (lowpass) to port 1 (common)

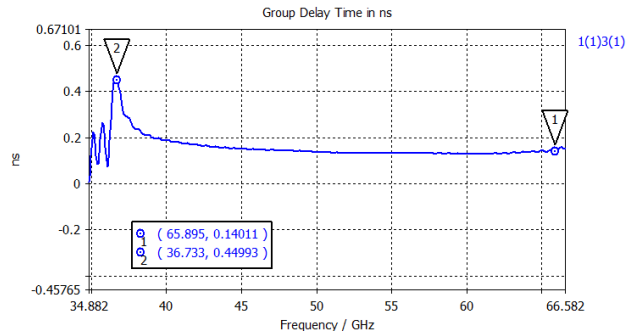

Fig. 14. Measured group delay from port 3 (highpass) to port 1 (common)

Excellent flatness and steep roll-off sharpness is achieved. Return loss better than 10 dB was measured across the band. Excellent correlation between simulated and measured results was achieved. Combining waveguide and SSL in the hybrid diplexer not only provides practical implementation capability but will also allow the extension of frequency performance of contiguous diplexers to W band and beyond.

Acknowledgment

The authors wish to acknowledge the mechanical design engineering support of Patrick Alladio, National Instruments, Santa Rosa CA.

References

[1] I. Ashiq and A. Khanna, "Ultra-Broadband Contiguous Planar DC-35-65 GHz Diplexer using Softboard Suspended Stripline Technology" IMS 2013, Seattle.

[2] A. Khanna and I. Ashiq, "Ultra-Broadband Diplexer Using Waveguide and Planar Transmission Lines," US Patent Application 6150-57100, Oct 2013

[3] Bhat and Koul, "Waveguide to Suspended Stripline Transition," Stripline-Like Transmission Lines for Microwave Integrated Circuits, New Age International, New Dehli 2007.

[4] P. Pupalaikis, B. Yamrone, R. Delbue, A.S. Khanna, K. Doshi, B. Bhat, and A. Sureka, "Technologies for Very High Bandwidth Real-time Oscilloscope," IEEE Bipolar/BiCMOS Circuits and Tech. Meetings (BCMT), Oct. 2014.